

A POSTERIORI ERROR ESTIMATES WITH BOUNDARY CORRECTION FOR A CUT FINITE ELEMENT METHOD

ERIK BURMAN ^{*}, CUIYU HE [†], AND MATS G. LARSON [‡]

Abstract. In this work we study a residual based a posteriori error estimation for the CutFEM method applied to an elliptic model problem. We consider the problem with non-polygonal boundary and the analysis takes into account the geometry and data approximation on the boundary. The reliability and efficiency are theoretically proved. Moreover, constants are robust with respect to how the domain boundary cuts the mesh.

Key words. CutFEM, A Posteriori Error Estimation, AMR

AMS subject classifications. 68Q25, 68R10, 68U05

1. Introduction. Meshing and re-meshing procedures remain an important challenge in computational methods, since they can be very computationally expensive for the finite element methods, particularly for problems with complex geometries and interfaces that move during the computational process. Several methods have been invented to alleviating the meshing procedure of the exact domain. Fictitious domain methods were introduced in the finite element context in the papers by Glowinski et al. [Glowinski & Pan \(1992\)](#) and unfitted finite element methods in the works by Barrett and Elliott [Barrett & Elliott \(1984\)](#).

Since these seminal works many approaches have been suggested on how to integrate the geometry data in finite element computations in a way that reduces the meshing effort. For instance the fat boundary method by Bertoluzza et al. [Bertoluzza et al. \(2005\)](#), the fictitious domain methods using Lagrange multipliers inspired by extended finite element methods, pioneered by Haslinger and Renard [Burman & Hansbo \(2010\)](#), [Haslinger & Renard \(2009\)](#), or the cut finite element method using Nitsche's method, introduced by Hansbo and Hansbo and further developed in the fictitious domain framework by various authors [Becker et al. \(2011\)](#), [Burman \(2010\)](#), [Burman & Hansbo \(2012\)](#), [Embar et al. \(2010\)](#), [Hansbo & Hansbo \(2002\)](#).

Cut finite element methods have been extensively studied in the recent years, both in the context of interface problems and for fictitious domain methods [Burman et al. \(2015b\)](#). We restrict the discussion herein to the fictitious domain case. The methodology alleviates the meshing process by employing a background mesh that can be highly structured and letting the domain boundary cut through the elements of the mesh. In cells cut by the boundary the equations are integrated only on the intersection of the element with the physical domain. The boundary conditions are then imposed either using Lagrange multipliers or Nitsche's method and stability with respect to the cut may be ensured using a ghost penalty stabilization [Burman \(2010\)](#). The method was originally designed for continuous approximation spaces, but has been adapted for various other methods, e.g. Discontinuous Galerkin method [Gürkan & Massing \(2019\)](#), [Johansson & Larson \(2013\)](#), Hybrid High order Methods [Burman & Ern \(2019\)](#) or Isogeometric analysis [Elfverson et al. \(2018\)](#). It has been

^{*}Department of Mathematics, University College London, Gower Street, London, UK-WC1E 6BT, United Kingdom (e.burman@ucl.ac.uk)

[†]Department of Mathematics, University College London, Gower Street, London, UK-WC1E 6BT, United Kingdom (c.he@ucl.ac.uk)

[‡]Department of Mathematics and Mathematical Statistics, Umeå University, SE-90187 Umeå, Sweden (mats.larson@umu.se)

applied to a number of different partial differential equations, e.g, incompressible elasticity/Stokes' equations [Burman & Hansbo \(2014\)](#), [Burman *et al.* \(2015a\)](#), [Guzmán & Olshanskii \(2018\)](#), [Massing *et al.* \(2014b\)](#), linear elasticity [Hansbo *et al.* \(2017\)](#), Helmholtz equations [Swift \(2018\)](#), time dependent parabolic problems on moving domains [Hansbo *et al.* \(2015\)](#), Oseen's problem [Massing *et al.* \(2018\)](#), [Winter *et al.* \(2018\)](#) and other fluid models [Schott & Wall \(2014\)](#), [Schott *et al.* \(2016\)](#). It has also been applied successfully to shape optimization problems [Bernland *et al.* \(2018\)](#), [Burman *et al.* \(2017, 2018b\)](#) and other advanced engineering applications [Bui *et al.* \(2019\)](#).

Typically, in cut finite element methods, a domain with curved boundary is approximated using a piecewise affine boundary approximation. This gives a sufficiently good geometry approximation for piecewise affine elements, but if higher order elements are used the geometry approximation must be improved. To alleviate the integration problem resulting from the elements cut by curved boundaries, isoparametric techniques [Lehrenfeld \(2017\)](#) and so called boundary value correction techniques have been proposed [Boiveau *et al.* \(2018\)](#), [Burman *et al.* \(2018a\)](#). For both these cases optimal order a priori error estimates for arbitrary order of the polynomial approximation have been derived. For an analysis of the fitted finite element method on domains with curved boundaries we refer to [Bramble & King \(1994\)](#).

The purpose of this paper is to design an a posteriori error estimation for the cut finite element method for problems with non-polygonal boundary. We will base our discussion on the cut finite element methods for the Poisson problem introduced by Burman and Hansbo [Burman & Hansbo \(2012\)](#). This method uses Nitsche's method [Nitsche \(1971\)](#) to impose Dirichlet boundary conditions and a ghost penalty term [Burman \(2010\)](#) to enhance stability in the boundary zone. We restrict the discussion to the fictitious domain problem and piecewise affine approximation. The main motivation for studying the a posteriori error estimation is for the application of adaptive mesh refinement (AMR) procedure. It is well known that AMR is extremely useful for problems with singularities, discontinuities, sharp derivatives, etc. and it has been extensively studied in the last two decades, [Ainsworth & Oden \(2011\)](#), [Verfürth \(1994\)](#). However, there is very limited work in the literature that takes the geometry approximation into account. In [Dörfler & Rumpf \(1998\)](#) the a posteriori error estimation is studied for the conforming finite element method on curved boundary where the boundary vertices of the approximated mesh must be located on the true boundary and it is assumed that data can be requested at any point on the boundary and inside the domain, i.e., there is only approximation of the geometry. In [Ainsworth & Rankin \(2017\)](#) a fully computable error bound is provided for the conforming linear elements with pure Neumann data. To the author's knowledge there is no existing work on the a posteriori error estimation for cut finite element methods on problems with curved boundary, to allow for. Another approach for the handling of geometric singularities in the cutFEM framework was recently proposed in [Jonsson *et al.* \(2019\)](#).

In our error analysis we do not assume that the vertices of the approximation boundary are located on the boundary of the continuous problem, while we do require that the discrete boundary is a sufficiently good approximation of the boundary of the continuous problem. We do not require that data inside the domain can be everywhere requested but only those originally provided in the continuous setting. For the formulation it is necessary to extend the source term data from the domain of the continuous problem to the computational domain, the extension must satisfy certain stability properties. The error estimator comprises two parts. One part is due to the numerical approximation; and the other part is exclusively due to the boundary

approximation. We refer to this latter contribution as the boundary correction error. This part must be computed using a locally improved boundary approximation in the boundary zone. The computation of this correction is discussed in the numerical section.

Unlike the methods whose mesh is an exact partition of the computational domain, one major challenge for cut finite element is that the approximated domain cuts the background mesh in an arbitrary way. Because of this the classical efficiency analysis, i.e., by applying the local elementary bubble functions, is not robust. Therefore we divide the efficiency part of the estimates in two parts. The residuals in the bulk, away from the boundary, are estimated in the ordinary fashion. For the residuals in the cut elements and the nonconforming ghost penalty operator, we instead prove a global lower bound of best approximation type, showing that the boundary residuals are bounded by the best approximation of u in the physical domain and oscillations.

This paper is organized as follows. In [section 2](#) the model problem and the cut finite element method is introduced. The error estimator is introduced in [section 3](#) and as well its global reliability. The local efficiency is proved in [section 4](#). Finally, we show the results of several numerical experiment in [section 5](#).

2. Model Problem and the Cut Finite Element Method.

2.1. The Continuous Problem. Let Ω be a domain in \mathbb{R}^d with Lipschitz continuous, piecewise smooth boundary $\partial\Omega$ and exterior unit normal \mathbf{n} .

We consider the problem: find $u : \Omega \rightarrow \mathbb{R}$ such that

$$(2.1) \quad -\Delta u = f \quad \text{in } \Omega$$

$$(2.2) \quad u = g \quad \text{on } \partial\Omega$$

where $f \in L^2(\Omega)$ and $g \in H^{1/2}(\partial\Omega)$ are given data. It follows from the Lax-Milgram lemma that there exists a unique solution $u \in H^1(\Omega)$ to this problem. We also have the following elliptic regularity estimate

$$(2.3) \quad \|u\|_{H^{s+2}(\Omega)} \lesssim \|f\|_{H^s(\Omega)}, \quad -1 \leq s \leq s_0$$

for some $s_0 \geq 1/2$ depending on the domain. Here and below we use the notation \lesssim to denote less or equal up to a generic constant that is independent of the mesh-geometry configuration.

2.2. The Mesh, Discrete Domains, and Finite Element Spaces. Assume that $\partial\Omega$ is composed of a finite number of smooth surfaces Γ_i , such that $\partial\Omega = \cup_i \bar{\Gamma}_i$. We let ρ be the signed distance function, negative on the inside and positive on the outside, to $\partial\Omega$ and we let $U_\delta(\partial\Omega)$, for $\delta > 0$, be the tubular neighborhood $\{\mathbf{x} \in \mathbb{R}^d : |\rho(\mathbf{x})| < \delta\}$ of $\partial\Omega$. Let $\Omega_0 \subset \mathbb{R}^d$ be a polygonal domain such that $U_{\delta_0}(\Omega) \subset \Omega_0$ where δ_0 is chosen such that ρ is well defined in $U_{\delta_0}(\Omega)$. Let $\mathcal{T}_{0,h}$ be a partition of Ω_0 into shape regular triangles or tetrahedra. Note that this setting allows meshes with locally dense refinement.

Given a subset ω of Ω_0 , let $\mathcal{T}_h(\omega)$ be the submesh defined by

$$(2.4) \quad \mathcal{T}_h(\omega) = \{K \in \mathcal{T}_{0,h} : \bar{K} \cap \bar{\omega} \neq \emptyset\}$$

i.e., the submesh consisting of elements that intersect $\bar{\omega}$, and let

$$(2.5) \quad \Delta_h(\omega) = \bigcup_{K \in \mathcal{T}_h(\omega)} K$$

be the union of all elements in $\mathcal{T}_h(\omega)$.

For each $\mathcal{T}_{0,h}$ let Ω_h be a polygonal domain approximating Ω and we assume that $\partial\Omega_h \subset U_{\delta_0}(\partial\Omega)$ which implies that $\partial\Omega_h$ is within the distance of δ_0 to $\partial\Omega$. We assume neither $\Omega_h \subset \Omega$ nor $\Omega \subset \Omega_h$, instead the maximum distance between the two domains has to be small enough.

Let the active mesh be defined by

$$(2.6) \quad \mathcal{T}_h := \mathcal{T}_h(\Omega \cup \Omega_h)$$

i.e., the submesh consisting of elements that intersect $\Omega_h \cup \Omega$, and let

$$(2.7) \quad \Delta_h := \Delta_h(\Omega \cup \Omega_h)$$

be the union of all elements in \mathcal{T}_h . Since $\partial\Omega_h$ does not necessarily fit the mesh we denote by \mathcal{T}_h^b the set of elements that are ‘‘cut’’ by $\partial\Omega_h$,

$$\mathcal{T}_h^b = \{K \in \mathcal{T}_{0,h} : K \cap \partial\Omega_h \neq \emptyset\} \subset \mathcal{T}_h.$$

We assume that Ω_h is constructed in such a way that for each $K \in \mathcal{T}_h^b$, the intersection $K \cap \partial\Omega_h$ is a subset of a $d - 1$ dimensional hyperplane, i.e., a line segment in two dimensions and a subset of a plane in three dimensions. Under the smallness assumption of h , for any element $K \in \mathcal{T}_h^b$ there exists an element $K' \in \mathcal{T}_h(\Omega_h) \setminus \mathcal{T}_h^b$ such that $\text{dist}(K, K') = O(h)$ where $O(\cdot)$ denotes the big ordo. This is always possible for small enough h since Ω is Lipschitz.

Also we denote by \mathcal{E} the set of all facets on \mathcal{T}_h and by $\mathcal{E}_I \subset \mathcal{E}$ the set of all interior facets with respect to \mathcal{T}_h . For each $F \in \mathcal{E}$ denote by \mathbf{n}_F an unit vector normal to F and by h_F the diameter of F . For each $K \in \mathcal{T}_h$ denote by h_K the diameter of K and by \mathcal{E}_K the set of all facets of K .

On the boundary $\partial\Omega_h$ let \mathbf{n}_h be the outer normal to $\partial\Omega_h$. For each Ω_h we assume that, for δ_0 small enough, there exist functions $\boldsymbol{\nu}_h : \partial\Omega_h \rightarrow \mathbb{R}^d$, $|\boldsymbol{\nu}_h| = 1$, and $\varrho_h : \partial\Omega_h \rightarrow \mathbb{R}$, on $U_{\delta_0}(\partial\Omega)$, such that the function $\mathbf{p}_h(\mathbf{x}, \varsigma) := \mathbf{x} + \varsigma\boldsymbol{\nu}_h(\mathbf{x})$, is well defined and satisfies $\mathbf{p}_h(\mathbf{x}, \varrho_h(\mathbf{x})) \in \partial\Omega$ for all $\mathbf{x} \in \partial\Omega_h$. The existence of the vector-valued function $\boldsymbol{\nu}_h$ is known to hold on Lipschitz domains, see Grisvard [Grisvard \(2011\)](#).

We further assume that $\mathbf{p}_h(\mathbf{x}, \varsigma) \in U_{\delta_0}(\Omega)$ for all $\mathbf{x} \in \partial\Omega_h$ and all ς between 0 and $\varrho_h(\mathbf{x})$. For conciseness we will drop the second argument, ς , of \mathbf{p}_h below whenever it takes the value $\varrho_h(\mathbf{x})$ and let \mathbf{p}_h denotes the map $\mathbf{p}_h : \partial\Omega_h \rightarrow \partial\Omega$. Moreover, we assume that the following assumption is satisfied

$$(2.8) \quad \|\varrho_h\|_{L^\infty(\partial\Omega_h \cap K)} \leq O(h_K) \quad \forall K \in \mathcal{T}_h^b.$$

The above assumption immediately implies that $\partial\Omega_h$ is within the distance of $O(h)$ of $\partial\Omega$. More precisely,

$$(2.9) \quad \|\varrho\|_{L^\infty(\partial\Omega_h \cap K)} = O(h_K) \quad \forall K \in \mathcal{T}_h^b.$$

This assumption is necessary for the constant in the a posteriori error estimates to be independent of the geometry/mesh configuration. It is however not enough to guarantee optimal a priori error estimates, which requires $\|\varrho\|_{L^\infty(\partial\Omega_h \cap K)} \leq O(h_K^2)$, and $\|\mathbf{n} - \mathbf{n}_h\|_{L^\infty(\partial\Omega_h \cap K)} \leq O(h_K)$, see [Burman et al. \(2018a\)](#).

2.3. The Cut Finite Element Method. In this subsection we recall the Cut-FEM introduced in [Burman & Hansbo \(2012\)](#). We begin with some necessary notation. Let \mathcal{F}_h be the set of faces intersecting the approximate boundary Ω_h :

$$\mathcal{F}_h = \{F \in \mathcal{E}_I : (K_F \cup K'_F) \cap \partial\Omega_h \neq \emptyset\}$$

where K_F and K'_F are those two elements sharing F as a common facet, and for any discontinuous function v define its jump on the facet F by

$$[[v]]|_F := v_F^+ - v_F^- \quad \text{and} \quad v_F^\pm(x) = \lim_{s \rightarrow 0^+} v(\mathbf{x} \mp s\mathbf{n}_F).$$

Next define the finite element space

$$(2.10) \quad V_h := \{v \in H^1(\Delta_h) : v|_K \in \mathbb{P}_1(K) \quad \forall K \in \mathcal{T}_h\}$$

and the forms

$$(2.11) \quad \begin{aligned} a_0(v, w) &:= (\nabla v, \nabla w)_{\Omega_h} - \langle D_{\mathbf{n}_h} v, w \rangle_{\partial\Omega_h} - \langle v, D_{\mathbf{n}_h} w \rangle_{\partial\Omega_h} + \sum_{K \in \mathcal{T}_h^b} \frac{\beta}{h_K} \langle v, w \rangle_{\Gamma_K}, \\ j_h(v, w) &:= \gamma \sum_{F \in \mathcal{F}_h} h_F \langle [[D_{\mathbf{n}_F} v]], [[D_{\mathbf{n}_F} w]] \rangle_F, \\ a_h(v, w) &:= a_0(v, w) + j_h(v, w), \\ l_h(w) &:= (f, w)_{\Omega_h} - \langle g_h, D_{\mathbf{n}_h} w \rangle_{\partial\Omega_h} + \sum_{K \in \mathcal{T}_h^b} \frac{\beta}{h_K} \langle g_h, w \rangle_{\Gamma_K}, \end{aligned}$$

where $D_{\mathbf{n}_h} v := \mathbf{n}_h \cdot \nabla v$, γ and β are positive constants, g_h is an approximation of g defined on $\partial\Omega_h$, typically $g_h(\mathbf{x}) = g \circ \mathbf{p}_h$, and $\Gamma_K = K \cap \partial\Omega_h$ and $f|_{\Omega_h \setminus \Omega}$ is defined by some suitable extension (in the low order case considered here it can be taken to be zero).

Remark 2.1. The stabilizing term $j_h(v, w)$, which is the so called ghost penalty term, is introduced to extend the coercivity of $a_h(\cdot, \cdot)$ to all of Δ_h , see [Burman \(2010\)](#), [Massing et al. \(2014a\)](#). Thanks to this property one may prove that the condition number of the linear system is uniformly bounded independent of how Ω_h is oriented compared to the mesh.

Remark 2.2. In order to guarantee the coercivity of (2.11) β has to be chosen large enough.

The finite element method is then to find $u_h \in V_h$ such that

$$(2.12) \quad a_h(u_h, v) = l_h(v) \quad \forall v \in V_h$$

where a_h and l_h are defined in (2.11).

For $v \in H^1(\Omega_0)$ define the continuous and discrete energy norm respectively by

$$(2.13) \quad \|v\|^2 := \|\nabla v\|_{\Omega}^2 + \|D_{\mathbf{n}} v\|_{H^{-1/2}(\partial\Omega)}^2 + \|h^{-\frac{1}{2}} v\|_{\partial\Omega}^2$$

and

$$(2.14) \quad \|v\|_h^2 := \|\nabla v\|_{\Omega_h}^2 + \sum_{K \in \mathcal{T}_h^b} h_K \|D_{\mathbf{n}_h} v\|_{\Gamma_K}^2 + \sum_{K \in \mathcal{T}_h^b} h_K^{-1} \|v\|_{\Gamma_K}^2.$$

2.4. Some Important Inequalities. We have the following well known inverse and trace inequalities (Di Pietro & Ern, 2012, Section 1.4.3),

$$(2.15) \quad \|v\|_{\partial K} \leq C(h_K^{-1/2}\|v\|_K + h_K^{1/2}\|\nabla v\|_K) \quad \forall v \in H^1(K),$$

$$(2.16) \quad h_K^{-\frac{1}{2}}\|v_h\|_{\partial K} + \|\nabla v_h\|_K \leq Ch_K^{-1}\|v_h\|_K \quad \forall v_h \in \mathbb{P}_1(K)$$

and Hansbo & Hansbo (2002)

$$(2.17) \quad \|v_h\|_{\Gamma_K} \leq C(h_K^{-1/2}\|v_h\|_K + h_K^{1/2}\|\nabla v_h\|_K) \quad \forall v_h \in \mathbb{P}_1(K)$$

where the constant C is independent of the relative location of Ω_h .

LEMMA 2.1. *Let $v \in H_0^1(\Omega)$. Then for any K such that $K \in \mathcal{T}_h^b$ or $K \cap (\Omega \setminus \Omega_h) \neq \emptyset$ there exists a local convex neighborhood \mathcal{S}_K of K such that v vanishes on a nonzero subset of $\partial\mathcal{S}_K$ and*

$$(2.18) \quad \|v\|_K \lesssim h_K \|\nabla v\|_{\mathcal{S}_K},$$

where we defined v outside Ω using the trivial extension $v|_{\Omega^c} = 0$.

Proof. If $K \subset \Omega^c$, the estimate (2.18) is obvious since v is taken uniformly zero outside Ω . If $K \cap \partial\Omega \neq \emptyset$, then we let $x \in K \cap \partial\Omega$ and let $S_K = B_\delta(x)$ be the open ball centered at x with radius $\delta \sim h$. The estimate (2.18) is a direct consequence of the Poincaré inequality on S_K . Otherwise $K \subset \Omega$. From (2.8) it follows that

$$\text{dist}(K, \partial\Omega) \leq O(h)$$

and thus there is $x \in \partial\Omega$ and $\delta \sim h$ such that $K \subset B_\delta(x)$ and now (2.18) follows with $S_K = B_\delta(x)$ from the Poincaré inequality on S_K . This completes the proof of the lemma. \square

3. Global Reliability. Let $e := u - u_h$ and \tilde{e} be any function such that

$$\tilde{e} \in H^1(\Omega) \quad \text{and} \quad \tilde{e}|_{\partial\Omega} = (g - u_h)$$

where u_h is the solution to (2.12).

For each element $K \in \mathcal{T}_h$, define the local element error indicator η_K by

$$(3.1) \quad \eta_K^2 = h_K^2 \|f\|_{K \cap \Omega_h}^2 + \sum_{F \in \mathcal{E}_K \cap \mathcal{E}_I} \frac{h_F}{2} \| [D_{\mathbf{n}_F} u_h] \|_F^2 + h_K^{-1} \|g_h - u_h\|_{L^2(\Gamma_K)}^2 + \|\nabla \tilde{e}\|_{K \cap \Omega}^2.$$

and let the global error estimator be defined by

$$(3.2) \quad \eta = \left(\sum_{K \in \mathcal{T}_h} \eta_K^2 \right)^{1/2}.$$

THEOREM 3.1. *Let $\tilde{e} \in H^1(\Omega)$ such that $\tilde{e}|_{\partial\Omega} = (g - u_h)|_{\partial\Omega}$. We have the following reliability bound*

$$(3.3) \quad \|\nabla e\|_\Omega \leq C_r \left(\sum_{K \in \mathcal{T}_h} \eta_K^2 + \sum_{K \in \mathcal{T}_h} h_K^2 \|f\|_{(\Omega \setminus \Omega_h) \cap K}^2 \right)^{1/2}$$

where the constant C_r does not depend on the location of domain-mesh intersection nor the mesh size.

Proof. Note that $e - \tilde{e} \in H_0^1(\Omega)$. By the triangle inequality we have that

$$\begin{aligned}
 \|\nabla e\|_\Omega &\leq \|\nabla(e - \tilde{e})\|_\Omega + \|\nabla \tilde{e}\|_\Omega \\
 &= \sup_{v \in H_0^1(\Omega)} \frac{(\nabla(e - \tilde{e}), \nabla v)_\Omega}{\|\nabla v\|_\Omega} + \|\nabla \tilde{e}\|_\Omega \\
 &\leq \sup_{v \in H_0^1(\Omega)} \frac{(\nabla e, \nabla v)_\Omega}{\|\nabla v\|_\Omega} + 2\|\nabla \tilde{e}\|_\Omega.
 \end{aligned}
 \tag{3.4}$$

It then suffices to show that

$$\sup_{v \in H_0^1(\Omega)} \frac{(\nabla e, \nabla v)_\Omega}{\|\nabla v\|_\Omega} \lesssim \left(\sum_{K \in \mathcal{T}_h} \eta_K^2 + \sum_{K \in \mathcal{T}_h} h_K^2 \|f\|_{(\Omega \setminus \Omega_h) \cap K}^2 \right)^{1/2},$$

which is a direct result from [Lemma 3.1](#) and [Lemma 3.2](#) below. This completes the proof of the theorem. \square

REMARK 3.1. *We omit the second term in (3.3) in the algorithm computation in order to avoid integration on the curved domain. What's more, one can easily make it a higher order term by satisfying*

$$\|\varrho\|_{L^\infty(\Gamma_K)} \leq o(h_K) \quad \forall K \in \mathcal{T}_h^b.$$

LEMMA 3.1. *For any $v \in H_0^1(\Omega)$ and $v_h \in V_h$ the following equality holds:*

$$(\nabla e, \nabla v)_\Omega = \mathcal{A}_1 + \mathcal{A}_2
 \tag{3.5}$$

where

$$\mathcal{A}_1 = (f, v - v_h)_{\Omega_h} + (f, v)_{\Omega \setminus \Omega_h}
 \tag{3.6}$$

and

$$\begin{aligned}
 \mathcal{A}_2 &= -\frac{1}{2} \sum_{K \in \mathcal{T}_h} \sum_{F \in \mathcal{E}_K} \int_{F \cap \Omega_h} \llbracket D_{\mathbf{n}_F} u_h \rrbracket (v - v_h) ds + \langle g_h - u_h, D_{\mathbf{n}_h} v_h \rangle_{\partial \Omega_h} \\
 &\quad - \frac{1}{2} \sum_{K \in \mathcal{T}_h} \sum_{F \in \mathcal{E}_K} \int_{F \cap (\Omega \setminus \Omega_h)} \llbracket D_{\mathbf{n}_F} u_h \rrbracket v ds \\
 &\quad - \sum_{K \in \mathcal{T}_h^b} \frac{\beta}{h_K} \langle g_h - u_h, v_h \rangle_{\Gamma_K} + j_h(u_h, v_h).
 \end{aligned}
 \tag{3.7}$$

Proof. Extending $v \in H_0^1(\Omega)$ to \mathbb{R}^d by setting $v = 0$ outside of Ω and using integration by parts gives

$$\begin{aligned}
 (\nabla e, \nabla v)_\Omega &= (f, v)_\Omega - (\nabla u_h, \nabla v)_{\Omega_h} - (\nabla u_h, \nabla v)_{\Omega \setminus \Omega_h} \\
 &= (f, v)_\Omega - (\nabla u_h, \nabla v_h)_{\Omega_h} - (\nabla u_h, \nabla(v - v_h))_{\Omega_h} - (\nabla u_h, \nabla v)_{\Omega \setminus \Omega_h}.
 \end{aligned}
 \tag{3.8}$$

For the second term in (3.8), by (2.12) we have

$$\begin{aligned}
 -(\nabla u_h, \nabla v_h)_{\Omega_h} &= -\langle D_{\mathbf{n}_h} u_h, v_h \rangle_{\partial \Omega_h} + j_h(u_h, v_h) - (f, v_h)_{\Omega_h} \\
 &\quad + \langle g_h - u_h, D_{\mathbf{n}_h} v_h \rangle_{\partial \Omega_h} - \sum_{K \in \mathcal{T}_h^b} \frac{\beta}{h_K} \langle g_h - u_h, v_h \rangle_{\Gamma_K}.
 \end{aligned}
 \tag{3.9}$$

For the last two terms in (3.8) applying the integration by parts gives

$$\begin{aligned}
& -(\nabla u_h, \nabla(v - v_h))_{\Omega_h} - (\nabla u_h, \nabla v)_{\Omega \setminus \Omega_h} \\
&= -\sum_{K \in \mathcal{T}_h} \int_{\partial(K \cap \Omega_h)} (D_{\mathbf{n}} u_h)(v - v_h) ds - \sum_{K \in \mathcal{T}_h} \int_{\partial(K \cap (\Omega \setminus \Omega_h))} (D_{\mathbf{n}} u_h)v ds \\
(3.10) \quad &= -\frac{1}{2} \sum_{K \in \mathcal{T}_h} \sum_{F \in \mathcal{E}_K} \int_{F \cap \Omega_h} \llbracket D_{\mathbf{n}_F} u_h \rrbracket (v - v_h) ds \\
&\quad - \frac{1}{2} \sum_{K \in \mathcal{T}_h} \sum_{F \in \mathcal{E}_K} \int_{F \cap (\Omega \setminus \Omega_h)} \llbracket D_{\mathbf{n}_F} u_h \rrbracket v ds + \langle D_{\mathbf{n}_h} u_h, v_h \rangle_{\partial \Omega_h}.
\end{aligned}$$

In the last equality we used the following identity

$$-\int_{\partial \Omega_h} \nabla u_h \cdot \mathbf{n} v ds - \int_{\partial(\Omega \setminus \Omega_h)} \nabla u_h \cdot \mathbf{n} v ds = 0$$

thanks to the fact that $v = 0$ on $\partial \Omega$ and in $\Omega_h \setminus \Omega$, where \mathbf{n} without subscript denotes the outer normal to the boundary of domain being integrated. The desired identity (3.5) is then a direct consequence of (3.8)–(3.10). This completes the proof of the lemma. \square

Remark 3.1. Note that \mathcal{A}_1 and \mathcal{A}_2 in Lemma 3.1 does not contain the inconsistency error caused by the boundary approximation. In other words, the boundary correction error has been independently isolated by the term $\|\nabla \tilde{e}\|$. Since any \tilde{e} satisfying the boundary condition will yield an upper bound for the error, an inappropriate construction of \tilde{e} will potentially over estimate the error.

LEMMA 3.2. *Let \mathcal{A}_1 and \mathcal{A}_2 be given in Lemma 3.1. Then we have the following estimates:*

$$(3.11) \quad \mathcal{A}_1 \lesssim \left(\sum_{K \in \mathcal{T}_h} \left(h_K^2 \|f\|_{K \cap \Omega_h}^2 + h_K^2 \|f\|_{K \cap (\Omega \setminus \Omega_h)}^2 \right) \right)^{1/2} \|\nabla v\|_{\Omega},$$

and

$$(3.12) \quad \mathcal{A}_2 \lesssim \left(\sum_{K \in \mathcal{T}_h} \sum_{F \in \mathcal{E}_K \cap \mathcal{E}_I} \frac{h_F}{2} \|\llbracket D_{\mathbf{n}_F} u_h \rrbracket\|_F^2 + \sum_{K \in \mathcal{T}_h^b} h_K^{-1} \|g_h - u_h\|_{\Gamma_K}^2 \right)^{1/2} \|\nabla v\|_{\Omega}.$$

Proof. The first term of \mathcal{A}_1 in (3.5) can be bounded directly using the Cauchy-Schwarz inequality and the approximation property of the Scott-Zhang interpolation Scott & Zhang (1990),

$$\begin{aligned}
(f, v - v_h)_{\Omega_h} &\leq \sum_{K \in \mathcal{T}_h} \|f\|_{K \cap \Omega_h} \|v - v_h\|_K \\
(3.13) \quad &\lesssim \sum_{K \in \mathcal{T}_h} h_K \|f\|_{K \cap \Omega_h} \|\nabla v\|_{\Delta_K} \\
&\lesssim \left(\sum_{K \in \mathcal{T}_h} h_K^2 \|f\|_{K \cap \Omega_h}^2 \right)^{1/2} \|\nabla v\|_{\Omega},
\end{aligned}$$

where Δ_K is the union of elements in \mathcal{T}_h that shares at least one vertex with K .

By (2.18) the second term of \mathcal{A}_1 can now be bounded as follows:

$$\begin{aligned}
 (f, v)_{\Omega \setminus \Omega_h} &\leq \sum_{K \in \mathcal{T}_h} \|f\|_{K \cap (\Omega \setminus \Omega_h)} \|v\|_{K \cap (\Omega \setminus \Omega_h)} \\
 (3.14) \quad &\lesssim \left(\sum_{K \in \mathcal{T}_h} h_K^2 \|f\|_{K \cap (\Omega \setminus \Omega_h)}^2 \right)^{1/2} \|\nabla v\|_{\Omega}.
 \end{aligned}$$

(3.11) is then a direct result of (3.13) and (3.14).

We now proceed to bound terms in \mathcal{A}_2 . The first term of \mathcal{A}_2 can be bounded directly by applying the Cauchy-Schwarz inequality and the approximation property of the Scott-Zhang interpolation,

$$\begin{aligned}
 & - \sum_K \sum_{F \in \mathcal{E}_K} \int_{F \cap \Omega_h} \llbracket D_{\mathbf{n}_F} u_h \rrbracket (v - v_h) ds \\
 & \leq \sum_K \sum_{F \in \mathcal{E}_K} \|\llbracket D_{\mathbf{n}_F} u_h \rrbracket\|_{F \cap \Omega_h} \|v - v_h\|_F \\
 (3.15) \quad & \lesssim \sum_K \sum_{F \in \mathcal{E}_K} h_K^{1/2} \|\llbracket D_{\mathbf{n}_F} u_h \rrbracket\|_{F \cap \Omega_h} \|\nabla v\|_{\Delta_K} \\
 & \lesssim \left(\sum_K \sum_{F \in \mathcal{E}_K} h_K \|\llbracket D_{\mathbf{n}_F} u_h \rrbracket\|_{F \cap \Omega_h}^2 \right)^{1/2} \|\nabla v\|_{\Omega}.
 \end{aligned}$$

To bound the second term in \mathcal{A}_2 we apply the trace inequality and (2.18) that

$$\begin{aligned}
 & - \sum_{K \in \mathcal{T}_h} \sum_{F \in \mathcal{E}_K} \int_{F \cap (\Omega \setminus \Omega_h)} \llbracket D_{\mathbf{n}_F} u_h \rrbracket v ds \\
 & \leq \sum_{K \in \mathcal{T}_h} \sum_{F \in \mathcal{E}_K} \|\llbracket D_{\mathbf{n}_F} u_h \rrbracket\|_{F \cap (\Omega \setminus \Omega_h)} \|v\|_F \\
 (3.16) \quad & \lesssim \sum_{K \in \mathcal{T}_h} \sum_{F \in \mathcal{E}_K} \|\llbracket D_{\mathbf{n}_F} u_h \rrbracket\|_{F \cap (\Omega \setminus \Omega_h)} \left(h_K^{-1/2} \|v\|_K + h_K^{1/2} \|\nabla v\|_K \right) \\
 & \lesssim \sum_{K \in \mathcal{T}_h} \sum_{F \in \mathcal{E}_K} h_K^{1/2} \|\llbracket D_{\mathbf{n}_F} u_h \rrbracket\|_{F \cap (\Omega \setminus \Omega_h)} \|\nabla v\|_{\mathcal{S}_K} \\
 & \lesssim \left(\sum_{K \in \mathcal{T}_h} \sum_{F \in \mathcal{E}_K} h_K \|\llbracket D_{\mathbf{n}_F} u_h \rrbracket\|_{F \cap (\Omega \setminus \Omega_h)}^2 \right)^{1/2} \|\nabla v\|_{\Omega}.
 \end{aligned}$$

The jump penalty term in \mathcal{A}_2 can be bounded by applying the Cauchy-Schwarz,

triangle, trace, and the inverse inequalities and the stability of the interpolator:

$$\begin{aligned}
j_h(u_h, v_h) &\leq \gamma \sum_{F \in \mathcal{F}_h} h_F \| [D_{\mathbf{n}_F} u_h] \|_F \| [D_{\mathbf{n}_F} v_h] \|_F \\
&\lesssim \sum_{F \in \mathcal{F}_h} h_F^{1/2} \| [D_{\mathbf{n}_F} u_h] \|_F \left(\sum_{K \in \{K_F^+, K_F^-\}} h_F^{1/2} \|\nabla v_h|_K\|_F \right) \\
(3.17) \quad &\lesssim \sum_{F \in \mathcal{F}_h} h_F^{1/2} \| [D_{\mathbf{n}_F} u_h] \|_F \left(\sum_{K \in \{K_F^+, K_F^-\}} \|\nabla v_h\|_K \right) \\
&\lesssim \sum_{F \in \mathcal{F}_h} h_F^{1/2} \| [D_{\mathbf{n}_F} u_h] \|_F \|\nabla v\|_{\Delta_F} \\
&\lesssim \left(\sum_{F \in \mathcal{F}_h} h_F \| [D_{\mathbf{n}_F} u_h] \|_F^2 \right)^{1/2} \|\nabla v\|_{\Omega},
\end{aligned}$$

where $K_F^+(K_F^-)$ is the element with $\mathbf{n}_F(-\mathbf{n}_F)$ being its outer unit normal on F and $\Delta_F := \Delta_{K_F^+} \cup \Delta_{K_F^-}$.

The remaining two terms in \mathcal{A}_2 can be bounded by applying the Cauchy-Schwarz and trace inequalities, (2.18) and the stability of the interpolator:

$$\begin{aligned}
&\sum_{K \in \mathcal{T}_h^b} \frac{\beta}{h_K} \langle g_h - u_h, v_h \rangle_{\Gamma_K} + \langle g_h - u_h, D_{\mathbf{n}_h} v_h \rangle_{\partial\Omega_h} \\
&\lesssim \sum_{K \in \mathcal{T}_h^b} (h_K^{-1} \|g_h - u_h\|_{\Gamma_K} \|v_h\|_{\Gamma_K} + \|g_h - u_h\|_{\Gamma_K} \|D_{\mathbf{n}_h} v_h\|_{\Gamma_K}) \\
(3.18) \quad &\lesssim \sum_{K \in \mathcal{T}_h^b} h_K^{-1} \|g_h - u_h\|_{\Gamma_K} \left(h_K^{-1/2} \|v_h\|_K + h_K^{1/2} \|\nabla v_h\|_K \right) \\
&\lesssim \sum_{K \in \mathcal{T}_h^b} h_K^{-1/2} \|g_h - u_h\|_{\Gamma_K} \|\nabla v\|_{\mathcal{S}_K \cup \Delta_K} \\
&\lesssim \left(\sum_{K \in \mathcal{T}_h^b} h_K^{-1} \|g_h - u_h\|_{\Gamma_K}^2 \right)^{1/2} \|\nabla v\|_{\Omega}.
\end{aligned}$$

Finally, combining (3.15)-(3.18) and the Young's inequality yields (3.12). This completes the proof of the lemma. \square

4. Efficiency. In this section we prove the efficiency of the error indicator introduced in (3.1). For the classical finite element method the efficiency is usually proved in a local fashion by applying the local facet and element bubble functions. For elements that are not intersected with the boundary and whose facets do not belong to the ghost penalty set we are able to prove the efficiency using the classical bubble technique.

LEMMA 4.1. *Let K be a given element in \mathcal{T}_h such that $K \notin \mathcal{T}_h^b$ and $\mathcal{E}_K \cap \mathcal{F}_h = \emptyset$. Then the following local efficiency result holds:*

$$(4.1) \quad \eta_K \leq C_\epsilon \|\nabla(u - u_h)\|_{\tilde{\Delta}_K},$$

where $\tilde{\Delta}_K$ is a local neighborhood of K and the efficiency constant C_e does not depend on the mesh size nor the domain-mesh intersection.

Proof. The proof is classical and we refer [Cai et al. \(2017\)](#), [Verfürth \(1994\)](#). \square

Remark 4.1. For the regular elements, we take the boundary correction error $\|\nabla \tilde{e}\|_{K \cap \Omega}$ to be 0 since we can always design \tilde{e} in such a way that it vanishes inside regular elements in order to avoid over-estimation (see [subsection 5.1](#)).

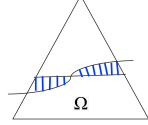


FIG. 1. An irregular element K and D_K (the shaded area)

For an element K that is irregular, i.e., $K \in \mathcal{T}_h^b$ or $\mathcal{E}_K \cap \mathcal{F}_h \neq \emptyset$, applying the same bubble technique for cut elements unfortunately will result in the dependence on the location of domain-mesh intersection. As an alternative we prove the efficiency for the term of ghost penalty as a whole. The efficiency bounds for the element residual on irregular elements can be then also proved with the aid of the efficiency result for the ghost penalty and the numerical scheme.

For each K define $E_K = \partial K \cap ((\Omega \cup \Omega_h) \setminus (\Omega \cap \Omega_h))$ and $D_K = K \cap ((\Omega \cup \Omega_h) \setminus (\Omega \cap \Omega_h))$, see [Figure 1](#) for an illustration.

We first prove a discrete Poincaré inequality that will be useful in the following efficiency proof.

LEMMA 4.2. *For any $v \in V_h$ the following estimate is true:*

$$(4.2) \quad \sum_{K \in \mathcal{T}_h} (h_K^{-2} \|v\|_{D_K}^2 + h_K^{-1} \|v\|_{E_K}^2) \lesssim \|v\|_h^2 + \|v_h\|_{j_h}^2,$$

where $\|v_h\|_{j_h}^2 = j_h(v_h, v_h)$.

Proof. First, for each K such that $E_K, D_K \neq \emptyset$, note that using the trace inequality [\(2.16\)](#) we see that

$$h_K^{-1} \|v\|_{E_K}^2 \leq h_K^{-1} \|v\|_{\partial K}^2 \lesssim h_K^{-2} \|v\|_K^2.$$

It follows that

$$h_K^{-2} \|v\|_{D_K}^2 + h_K^{-1} \|v\|_{E_K}^2 \lesssim h_K^{-2} \|v\|_K^2.$$

Now observe that there exists a set denoted by $S_K \subset \Delta_h$ such that $E_K, D_K \subset S_K$, $\text{diam}(S_K \cap \Omega_h)$ is of order h_K and for which using Poincaré's inequality

$$(4.3) \quad \|v\|_K \lesssim h_K \|\nabla v\|_{S_K} + \sum_{K' \cap S_K \neq \emptyset} h_{K'}^{1/2} \|v\|_{\Gamma_{K'}}.$$

By the equivalence of norms theorem we also have

$$(4.4) \quad \|\nabla v\|_{S_K} \leq \|\nabla v\|_{S_K \cap \Omega_h} + \sum_{\substack{F \in \mathcal{E}_I \\ F \subset S_K}} h_F^{1/2} \| [D_{\mathbf{n}_F} v] \|_F.$$

Combining [\(4.3\)](#) and [\(4.4\)](#) gives [\(4.2\)](#). This completes the proof of the lemma. \square

We assume that for each $K \in \mathcal{T}_h^b$ there exists at least one vertex, say z , of K such that $\text{diam}(\omega_z \cap \Omega_h) = O(h_K)$ where ω_z is the union of all elements sharing z as a vertex. Define

$$\text{osc}(f) = \sum_K \left(h_K^2 \|f - f_z\|_{\omega_z \cap \Omega_h}^2 + h_K^2 \|f - f_z\|_{K \cap (\Omega \setminus \Omega_h)}^2 \right)^{1/2},$$

where f_z is chosen such that $f_z = \text{argmin}_{c \in \mathcal{R}} h_K \|f - c\|_{\omega_z \cap \Omega_h}$. We will now proceed and prove a best approximation result for the element residuals of the cut elements. First we give a Lemma showing that the element residual of a cut element can be bounded by the ghost penalty term, the boundary residual and oscillation in data.

LEMMA 4.2. *For each $K \in \mathcal{T}_h^b$ its element residual has the following bound:*

$$(4.5) \quad h_K \|f\|_{K \cap \Omega_h} \lesssim \sum_{F \subset \bar{\omega}_z \cap \mathcal{E}_I} h_F^{1/2} \|[[D_{\mathbf{n}_F} u_h]]\|_{F \cap \Omega_h} + \left(\sum_{K' \subset \omega_z} h_{K'}^{-1} \|u_h - g_h\|_{\Gamma_{K'}}^2 \right)^{\frac{1}{2}} + h_K \|f - f_z\|_{\omega_z \cap \Omega_h} + h_K \|f - f_z\|_{K \cap (\Omega \setminus \Omega_h)}.$$

Proof. By the triangle inequality we firstly have

$$(4.6) \quad h_K \|f\|_{K \cap \Omega_h} \leq h_K \|f - f_z\|_{K \cap \Omega_h} + h_K \|f_z\|_{\omega_z \cap \Omega_h},$$

where f_z at this point can be chosen as any arbitrary constant. Let λ_z be the barycentric hat function associated with z then we also have

$$(4.7) \quad \|f_z\|_{\omega_z \cap \Omega_h}^2 \lesssim \|f_z \lambda_z^{1/2}\|_{\Omega_h}^2 = (f, f_z \lambda_z)_{\Omega_h} - (f - f_z, f_z \lambda_z)_{\Omega_h}.$$

Let $w_z = f_z \lambda_z$. Applying (2.12) and integration by parts yields

$$(4.8) \quad \begin{aligned} & (f, f_z \lambda_z)_{\Omega_h} = (\nabla u_h, \nabla w_z)_{\Omega_h} - \langle D_{\mathbf{n}_h} u_h, w_z \rangle_{\partial \Omega_h} - \langle u_h - g_h, D_{\mathbf{n}_h} w_z \rangle_{\partial \Omega_h} \\ & + \sum_{K' \in \mathcal{T}_h^b} \frac{\beta}{h_{K'}} \langle u_h - g_h, w_z \rangle_{\Gamma_{K'}} + \gamma \sum_{F \in \mathcal{F}_h} h_F \langle [[D_{\mathbf{n}_F} u_h]], [[D_{\mathbf{n}_F} w_z]] \rangle_F \\ = & \sum_{F \subset \omega_z} \langle [[D_{\mathbf{n}_F} u_h]], w_z \rangle_{F \cap \Omega_h} - \langle u_h - g_h, D_{\mathbf{n}_h} w_z \rangle_{\partial \Omega_h} \\ & + \sum_{K' \in \mathcal{T}_h^b} \frac{\beta}{h_{K'}} \langle u_h - g_h, w_z \rangle_{\Gamma_{K'}} + \gamma \sum_{F \in \mathcal{F}_h} h_F \langle [[D_{\mathbf{n}_F} u_h]], [[D_{\mathbf{n}_F} w_z]] \rangle_{F \cap \bar{\omega}_z} \\ \lesssim & \sum_{F \subset \omega_z} h_F^{-1/2} \|[[D_{\mathbf{n}_F} u_h]]\|_{F \cap \Omega_h} \|f_z\|_{\omega_z \cap \Omega_h} + \sum_{\substack{K' \subset \omega_z \\ K' \in \mathcal{T}_h^b}} h_{K'}^{-3/2} \|u_h - g_h\|_{\Gamma_{K'}} \|f_z\|_{\omega_z \cap \Omega_h} \\ & + \sum_{\substack{F \in \mathcal{F}_h \\ F \subset \bar{\omega}_z}} h_F^{-1/2} \|[[D_{\mathbf{n}_F} u_h]]\|_{F \cap \bar{\omega}_z} \|f_z\|_{\omega_z \cap \Omega_h}. \end{aligned}$$

The last inequality utilizes the fact that f_z is a constant and the trace and inverse inequalities. Combining (4.7), (4.8) and the Cauchy Schwarz inequality gives

$$(4.9) \quad \begin{aligned} h_K \|f_z\|_{\Omega_h \cap K} & \lesssim \sum_{F \subset \bar{\omega}_z \cap \mathcal{E}_I} h_F^{1/2} \|[[\nabla u_h \cdot \mathbf{n}_F]]\|_F \\ & + \left(\sum_{K' \subset \omega_z} h_{K'}^{-1} \|u_h - g_h\|_{\Gamma_{K'}}^2 \right)^{\frac{1}{2}} + \|f - f_z\|_{\omega_z \cap \Omega_h}, \end{aligned}$$

which, combining with (4.6), yields (4.5). \square

We now prove the main bound for the residuals in the cut elements.

THEOREM 4.1. *Let u and u_h be the solution to (2.1) and (2.12), respectively. Then the following best approximation result holds:*

$$(4.10) \quad \begin{aligned} & j_h(u_h, u_h) + \sum_{K \in \mathcal{T}_h^b} h_K^2 \|f\|_{K \cap \Omega_h}^2 \\ & \leq C_e \inf_{v_h \in V_h} \left(\| \|u - v_h\| \|^2 + \| \|v_h\| \|_{j_h}^2 + \sum_{K \in \mathcal{T}_h^b} h_K^{-1} \|v_h - g_h\|_{\Gamma_K}^2 + \text{osc}(f)^2 \right). \end{aligned}$$

where the constant C_e does not depend on the mesh size nor on the domain-mesh intersection.

Proof. By the triangle inequality we have

$$(4.11) \quad j_h(u_h, u_h) \lesssim j_h(u_h - v_h, u_h - v_h) + j_h(v_h, v_h)$$

and

$$(4.12) \quad \sum_{K \in \mathcal{T}_h^b} h_K^{-1} \|u_h - g_h\|_{\Gamma_K}^2 \lesssim \sum_{K \in \mathcal{T}_h^b} h_K^{-1} \|u_h - v_h\|_{\Gamma_K}^2 + \sum_{K \in \mathcal{T}_h^b} h_K^{-1} \|v_h - g_h\|_{\Gamma_K}^2$$

Denote by $\phi = u_h - v_h$. Then

$$j_h(u_h - v_h, u_h - v_h) + \sum_{K \in \mathcal{T}_h^b} h_K^{-1} \|u_h - v_h\|_{\Gamma_K}^2 \leq \| \phi \| \| \phi \|_h^2 + \| \phi \| \| \phi \|_{j_h}^2.$$

Applying the coercivity result (see Burman *et al.* (2015b)), (2.11) and (2.12) gives

$$(4.13) \quad \begin{aligned} & \| \phi \| \| \phi \|_h^2 + \| \phi \| \| \phi \|_{j_h}^2 \lesssim j_h(u_h - v_h, \phi) + a_0(u_h - v_h, \phi) \\ & = l_h(\phi) - a_0(v_h, \phi) - j_h(v_h, \phi) \\ & = l_h(\phi) - (f, \phi)_\Omega + (\nabla u, \nabla \phi)_\Omega - \langle D_{\mathbf{n}} u, \phi \rangle_{\partial \Omega} - a_h(v_h, \phi) - j_h(v_h, \phi) \\ & \triangleq \sum_{i=1}^4 \mathcal{A}_i, \end{aligned}$$

where

$$\begin{aligned} \mathcal{A}_1 &= (f, \phi)_{\Omega_h} - (f, \phi)_\Omega, \\ \mathcal{A}_2 &= \langle v_h - g_h, \nabla \phi \cdot \mathbf{n} \rangle_{\partial \Omega_h} - \sum_{K \in \mathcal{T}_h^b} \frac{\beta}{h_K} \langle v_h - g_h, \phi \rangle_{\Gamma_K}, \\ \mathcal{A}_3 &= (\nabla u, \nabla \phi)_\Omega - (\nabla v_h, \nabla \phi)_{\Omega_h} + \langle D_{\mathbf{n}_h} v_h, \phi \rangle_{\partial \Omega_h} - \langle D_{\mathbf{n}} u, \phi \rangle_{\partial \Omega}, \\ \mathcal{A}_4 &= -j_h(v_h, \phi). \end{aligned}$$

To estimate \mathcal{A}_1 , applying the Cauchy-Schwarz inequality and Lemma 4.2 gives

$$(4.14) \quad \begin{aligned} \mathcal{A}_1 & \leq \left(\sum_{K \in \mathcal{T}_h} h_K^2 \|f\|_{D_K}^2 \right)^{1/2} \left(\sum_{K \in \mathcal{T}_h} h_K^{-2} \|\phi\|_{D_K}^2 \right)^{1/2} \\ & \lesssim \left(\sum_{K \in \mathcal{T}_h} h_K^2 \|f\|_{D_K}^2 \right)^{1/2} (\| \phi \| \| \phi \|_h + \| \phi \| \| \phi \|_{j_h}). \end{aligned}$$

\mathcal{A}_2 can be estimated directly using the Cauchy-Schwarz inequality,

$$(4.15) \quad \begin{aligned} \mathcal{A}_2 &\leq \left(\sum_{K \in \mathcal{T}_h^b} h_K^{-1} \|v_h - g_h\|_{\Gamma_K}^2 \right)^{1/2} \left(\sum_{K \in \mathcal{T}_h^b} h_K \|D_{\mathbf{n}_h} \phi\|_{\Gamma_K}^2 + \sum_{K \in \mathcal{T}_h^b} h_K^{-1} \|\phi\|_{\Gamma_K}^2 \right)^{1/2} \\ &\lesssim \left(\sum_{K \in \mathcal{T}_h^b} h_K^{-1} \|v_h - g_h\|_{\Gamma_K}^2 \right)^{1/2} \|\phi\|_h \end{aligned}$$

To estimate \mathcal{A}_3 , add and subtract suitable terms to obtain,

$$\begin{aligned} \mathcal{A}_3 &= (\nabla(u - v_h), \nabla\phi)_\Omega - \langle \nabla(u - v_h) \cdot \mathbf{n}, \phi \rangle_{\partial\Omega} \\ &\quad + (\nabla v_h, \nabla\phi)_{\Omega \setminus \Omega_h} - (\nabla v_h, \nabla\phi)_{\Omega_h \setminus \Omega} + \langle \nabla v_h \cdot \mathbf{n}, \phi \rangle_{\partial\Omega_h} - \langle \nabla v_h \cdot \mathbf{n}, \phi \rangle_{\partial\Omega}. \end{aligned}$$

Observe that using integration by parts we have

$$\begin{aligned} &(\nabla v_h, \nabla\phi)_{\Omega \setminus \Omega_h} - (\nabla v_h, \nabla\phi)_{\Omega_h \setminus \Omega} + \langle \nabla v_h \cdot \mathbf{n}, \phi \rangle_{\partial\Omega_h} - \langle \nabla v_h \cdot \mathbf{n}, \phi \rangle_{\partial\Omega} \\ &\leq \sum_{K \in \mathcal{T}_h^b} \int_{E_K} \|[D_{\mathbf{n}_F} v_h]\phi\| ds \\ &\leq j_h(v_h, v_h)^{\frac{1}{2}} \left(\sum_{K \in \mathcal{T}_h^b} \|h^{-\frac{1}{2}} \phi\|_{E_K}^2 \right)^{\frac{1}{2}} \\ &\leq j_h(v_h, v_h)^{\frac{1}{2}} (\|\phi\|_h + \|\phi\|_{j_h}) \end{aligned}$$

where we used Lemma 4.2 for the last inequality. Then applying the Cauchy-Schwarz inequality and Lemma 4.2 gives

$$(4.16) \quad \begin{aligned} \mathcal{A}_3 &\leq \|\nabla(u - v_h)\|_\Omega \|\nabla\phi\|_\Omega + \|D_{\mathbf{n}_h}(u - v_h)\|_{H^{-1/2}(\partial\Omega)} \|\phi\|_{H^{1/2}(\partial\Omega)} \\ &\quad + j_h(v_h, v_h)^{\frac{1}{2}} (\|\phi\|_h + \|\phi\|_{j_h}) \\ &\leq (\|\nabla(u - v_h)\|_\Omega + \|D_{\mathbf{n}_h}(u - v_h)\|_{H^{-1/2}(\partial\Omega)} + j_h(v_h, v_h)^{\frac{1}{2}}) (\|\phi\|_h + \|\phi\|_{j_h}). \end{aligned}$$

Here we also used the inequality

$$\|\phi\|_{H^{1/2}(\partial\Omega)} \lesssim \|\phi\|_{H^1(\Omega)} \lesssim \|\phi\|_h + \|\phi\|_{j_h}.$$

Collecting the bounds (4.13)–(4.16) we see that

$$(4.17) \quad \|\phi\|_h + \|\phi\|_{j_h} \lesssim \inf_{v_h \in V_h} (\|\nabla(u - v_h)\|_\Omega + \|D_{\mathbf{n}_h}(u - v_h)\|_{H^{-1/2}(\partial\Omega)} + j_h(v_h, v_h)^{\frac{1}{2}})$$

Finally, combining Lemma 4.2, (4.11), (4.12) and (4.17) yields (4.10). This completes the proof of the theorem. \square

Remark 4.3. Regarding the efficiency for the indicator of the boundary correction error, we have the following efficiency result:

$$\inf_{\substack{\tilde{e} \in H^1(\Omega) \\ \tilde{e} = g - u_h \text{ on } \partial\Omega}} \|\nabla \tilde{e}\| = \|u - u_h\|_{H^{1/2}(\partial\Omega)} \lesssim \|u - u_h\|.$$

This also indicates that \tilde{e} needs to be designed properly to avoid over estimation. In section 5 we propose an approach to design and compute \tilde{e} .

5. Numerical Results. In this section we present several numerical examples to validate the performance of the a posteriori error estimator in the adaptive mesh refinement procedure. The adaptive mesh refinement procedure is set as follows:

Solve \rightarrow Estimate \rightarrow Mark \rightarrow Refine \rightarrow Solve.

For the penalty parameters in the finite element method, we set $\beta = 10$ and $\gamma = 0.1$. For the refinement strategy, we use the Dörfler marking strategy and the refine rate is set to be ten percent. Regarding the domain approximation, for a given ϕ being the level set function that satisfies $\phi = 0$ on the boundary and negative (positive) inside (outside) the domain Ω , let ϕ_h be the nodal interpolation of ϕ with respect to \mathcal{T}_h . And we define

$$(5.1) \quad \partial\Omega_h = \{\mathbf{x} : \phi_h(\mathbf{x}) = 0\}.$$

5.1. Computation of $\|\nabla\tilde{e}\|_\Omega$. In this subsection we introduce one way to compute the boundary correction error $\|\nabla\tilde{e}\|_\Omega$. We firstly construct a boundary correction mesh, denoted by \mathcal{T}_h^{bc} , which is finer than the current mesh \mathcal{T}_h in order to more accurately track the boundary $\partial\Omega$. More precisely, the new mesh is built inside the union of all intersection elements, i.e.,

$$\cup_{K \in \mathcal{T}_h^{bc}} K \subset \cup_{K \in \mathcal{T}_h^b} K.$$

For each element $K \in \mathcal{T}$, without loss of generality, in two dimensions, we assume that $\phi(z_0) \leq \phi(z_1) \leq \phi(z_2)$ where $z_i, i = 0, 1, 2$ are vertices of K . For each $K \in \mathcal{T}_h^b$ we assume the following must be true: there exists at least one facet in K such that the nodes connected to that facet have both positive and negative values, i.e.,

$$\phi(z_0) < 0 \quad \text{and} \quad \phi(z_2) > 0.$$

We then further partition the elements in \mathcal{T}_h^b based on the intersection of the domain and the mesh. The pseudo code for the algorithm is provided in [Algorithm 5.1](#). An example boundary correction mesh for Example 1 is shown in [Figure 3](#).

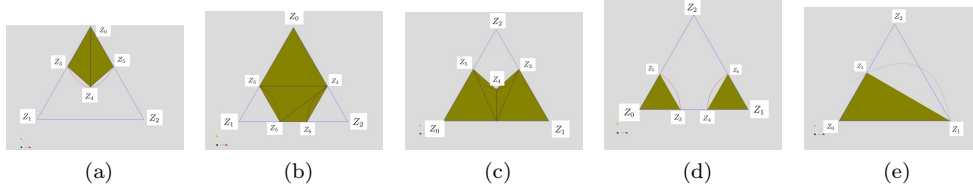


FIG. 2. Partition of the intersection cell based on the cut of level set.

With the mesh \mathcal{T}_h^{bc} available, we define \tilde{e} to be a piecewise linear conforming function with respect to \mathcal{T}_h^{bc} such that

$$\tilde{e}(z) = \begin{cases} g(z) - u_h(z) & \text{if } z \in \partial\Omega, \\ 0 & \text{otherwise.} \end{cases}$$

Algorithm 5.1 Build the boundary correction mesh in two dimensions

```

for cell  $K \in \mathcal{T}_h^b$  do
  if  $\phi(z_1) > 0$  then
    if  $\phi((z_1 + z_2)/2) \geq 0$  then
      Set Type as 'a'
      Find intersection points  $z_3$ - $z_5$  and form 2 triangles as as shown in Figure 2a
    else
      Set Type as 'b'
      Find intersection points  $z_3$ - $z_6$  and form 4 triangles as as in Figure 2b
    end if
  else if  $\phi(z_1) < 0$  then
    if  $\phi((z_0 + z_1)/2) < 0$  then
      Set Type as 'c'
      Find intersection points  $z_3$ - $z_5$  and form 4 triangles as as shown in Figure 2c
    else
      Set Type as 'd'
      Find intersection points  $z_3$ - $z_6$  and form 2 triangles as as in Figure 2d
    end if
  else
    Set Type as 'e'
    Find intersection point  $z_3$  and form 1 triangle as in in Figure 2e
  end if
end for

```

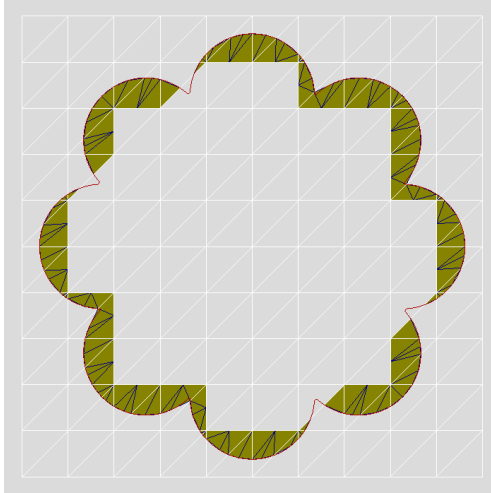


FIG. 3. An example of the boundary correction mesh for Example 1

Remark 5.1. It is critical that \tilde{e} is properly designed so that the boundary correction does not over-estimate the error due to the underresolved geometry. In our construction, it is easy to see that $\tilde{e} = \tilde{g} - u_h$ on $\partial\Omega$ where \tilde{g} is the nodal interpolation of g with respect to \mathcal{T}_h^{bc} on $\partial\Omega$. Then we have that

$$\|\tilde{g} - u_h\|_{1/2, \partial\Omega} \leq \|\nabla \tilde{e}\|_{\Omega} \lesssim \|\tilde{g} - u_h\|_{1/2, \partial\Omega}.$$

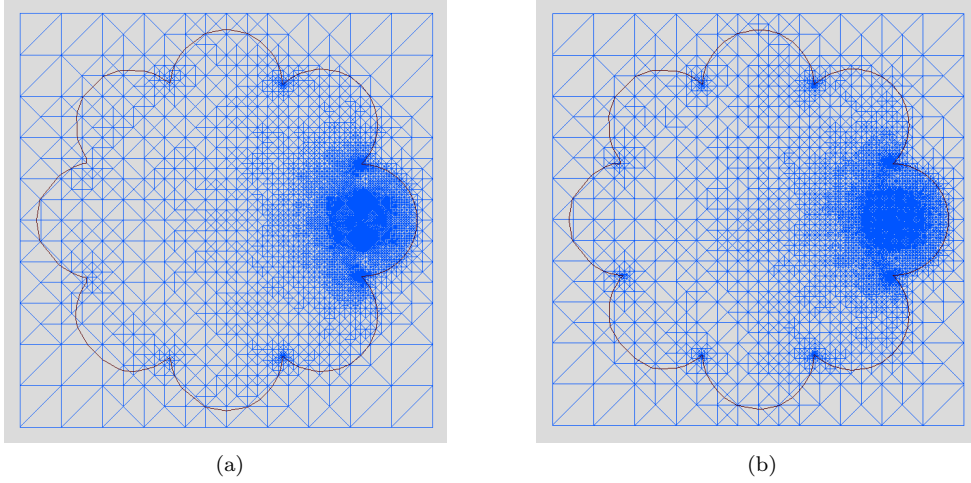


FIG. 4. Final meshes generated without and with $\|\nabla\bar{e}\|_K$.

The second inequality follows from the equivalence of norms.

5.2. Numerical Examples.

EXAMPLE 5.1. The level set of the problem has a flower shape (see Figure 3) that has the following representation:

$$\phi = \min(\phi_0, \phi_1, \dots, \phi_8)$$

with

$$\begin{cases} \phi_0(x, y) = x^2 + y^2 - r^2, & r = 2 \\ \phi_i(x, y) = (x - x_i)^2 + (y - y_i)^2 - r_i^2, & r_i = \sqrt{2}r * (\sin(\pi/8) + \cos(\pi/8)) \sin(\pi/8) \end{cases}$$

for $i = 1, \dots, 8$, $x_i = r(\cos(\pi/8) + \sin(\pi/8)) \cos(i * \pi/4)$ and $y_i = r(\cos(\pi/8) + \sin(\pi/8)) \sin(i * \pi/4)$. The domain Ω is defined as $x \in \mathbb{R}^2$ such that $\phi(x) \leq 0$. The data are given such that $g = 0$ on $\partial\Omega$ and

$$f(x, y) = \begin{cases} 10 & \text{if } (x - x_1)^2 + (y - y_1)^2 \leq r_1^2/2. \\ 0 & \text{otherwise.} \end{cases}$$

In the numerical scheme, we take $g_h = 0$. With the stopping criteria that the total number of degree of freedoms be not greater than 7000, the final meshes obtained without and with adding the boundary correction term are given $\|\nabla\bar{e}\|$ in Figure 4a and Figure 4b, respectively. We observe that slightly more degree of freedoms are added around the concave corners in Figure 4b. The corresponding convergence performances of each adaptive procedure are given in Figure 5. We observe that both estimators converge optimally when the mesh become fine enough. Adding the boundary correction term does slightly increases the estimator at the initial stage. However, the weight is diminishing as the mesh gets finer.

EXAMPLE 5.2. The level set of this problem has the following representation:

$$\phi = \max(\phi_0, -\phi_1, \dots, -\phi_8)$$

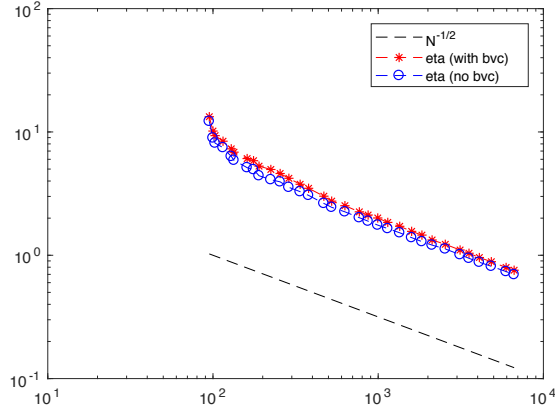


FIG. 5. Estimator convergence rate without and with $\|\nabla\tilde{e}\|$

with ϕ_0 to ϕ_8 defined the same as in [Example 5.1](#). The datum are chosen such that

$$f = 0 \quad \text{and} \quad g = y^2.$$

In the numerical scheme we approximate the boundary by Ω_h defined in [\(5.1\)](#). For the Dirichlet datum we take g_h to be the conforming piecewise linear interpolation of $g = y^2$. With the stopping criteria that the total number of degree of freedoms be not greater than 7000, the final meshes obtained without and with adding the boundary correction term $\|\nabla\tilde{e}\|_K$ are given in [Figure 6a](#) and [Figure 6b](#), respectively. The corresponding convergence performance of each adaptive procedure are given in [Figure 7](#). We observe that in both cases the estimator converges optimally. In [Figure 6b](#) note that there is no more obvious dense refinement comparing to [Figure 6a](#) around the boundary including the corners since in this case the approximation error $g - g_h$ is of uniform order everywhere.

5.3. Example 3. In this example we consider the reentrant problem whose solution has the following polar representation:

$$u(r, \theta) = r^\alpha \sin(\alpha\theta),$$

with $\alpha = \pi/\omega$ and ω being the angle of the reentrant corner. In this example, we test two values for ω , i.e., $31\pi/8$ and $63\pi/16$. The stopping criteria is set such that the maximal number of degrees of freedom does not exceed 5000. In the numerical scheme we approximate the Dirichlet datum g by g_h using conforming piecewise linear interpolation. The final meshes generated without adding the boundary correction error are given in [Figure 8a–Figure 8b](#) and with the boundary correction error are given in [Figure 9a–Figure 9b](#). The corresponding convergence rate of estimators are presented in [Figure 10a–Figure 10b](#). We again observe the optimal convergence performance for the estimator and true error in all cases. This indicates that the estimator, with or without the boundary correction error, works equivalently effective for problem even with singularity on the boundary.

We now test the same procedure but with g_h to be the piecewise constant interpolation of g for $w = 31\pi/16$. From the final meshes generated in [Figure 11a](#) and

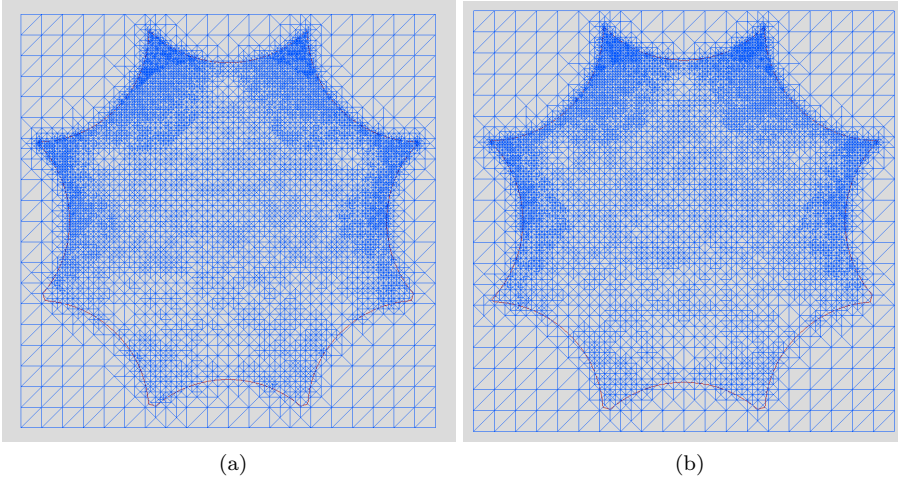


FIG. 6. Final meshes generated without and with $\|\nabla\tilde{e}\|_K$.

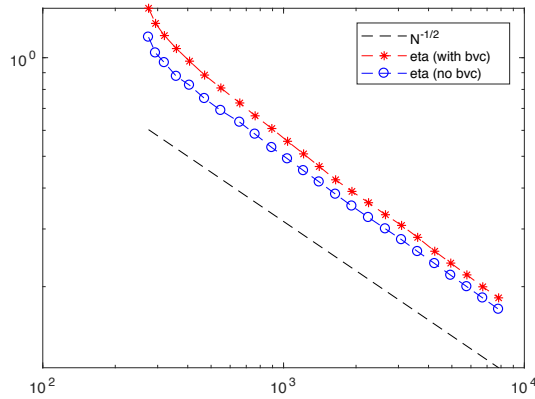


FIG. 7. estimator convergence rate without and with $\|\nabla\tilde{e}\|$

Figure 11b we observe that more degree of freedoms are added around the boundary in both cases due to the poorer approximation of the boundary data. The estimators, however, still converges optimally in both cases when the meshes are fine enough.

5.4. Example 4. In this example, we consider the problem that has the following representation:

$$u(x, y) = r^\alpha \sin(\alpha\theta) + \exp(100 * ((x - 0.5)^2 + (y - 0.5)^2))$$

with $r = \sqrt{x^2 + y^2}$, $\theta = \tan^{-1}(y/x)$, $\alpha = \pi/\omega$ and $\omega = 31\pi/16$. This problem has multiple singularities with one reentrant corner at $(0,0)$ and one peak at $(0.5, 0.5)$. In the numerical scheme, g_h and f_h are taken as the linear nodal interpolation of g and f , respectively. The stopping criteria is set to not exceed the maximal refinement step of 50 and the maximal number of degrees of freedom of 7500. The final meshes are given in Figure 13a and Figure 13b and their corresponding convergence performance

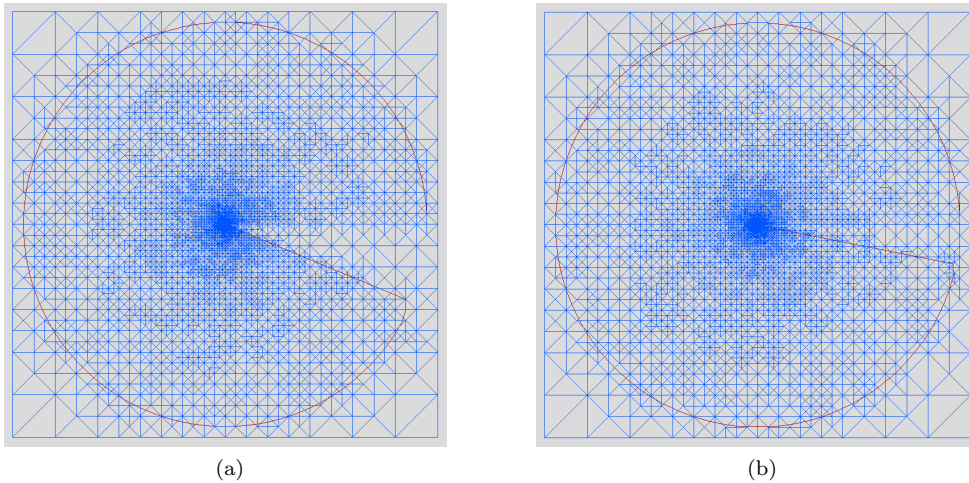


FIG. 8. Final meshes generated without $\|\nabla\tilde{e}\|_K$. Left: $\omega = 31\pi/8$. Right: $\omega = 63\pi/16$.

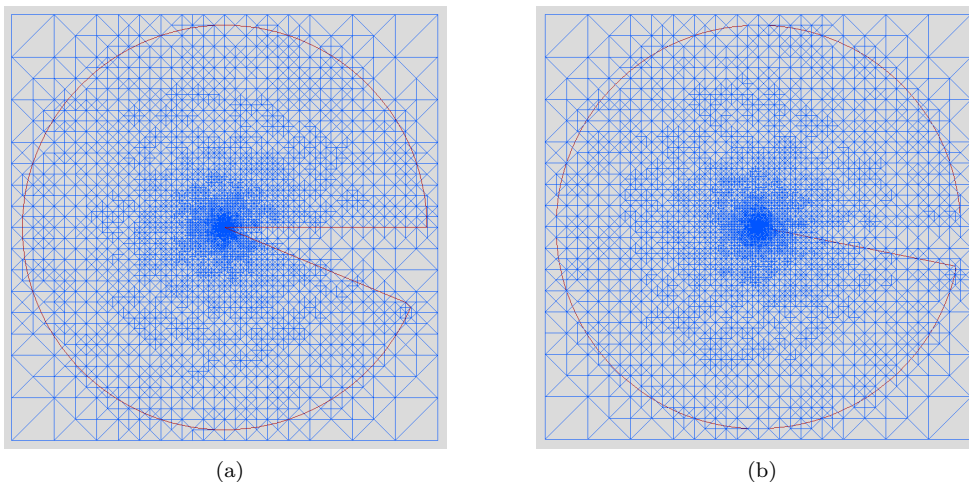


FIG. 9. Final meshes generated with $\|\nabla\tilde{e}\|_K$. Left: $\omega = 31\pi/8$. Right: $\omega = 63\pi/16$.

are presented in [Figure 14](#).

This example shows that the algorithm works also effectively when multiple singularities occurs, no matter the singularity happens on the boundary or inside the domain.

Acknowledgement. EB and CH were supported by EPSRC, UK, Grant No. EP/P01576X/1. ML was supported by the Swedish Foundation for Strategic Research Grant No. AM13-0029, the Swedish Research Council Grants No. 2017-03911, and the Swedish strategic research programme eSSSENCE.

References.

- Ainsworth, Mark, & Oden, J Tinsley. 2011. *A posteriori error estimation in finite element analysis*. Vol. 37. John Wiley & Sons.
- Ainsworth, Mark, & Rankin, Richard. 2017. Computable error bounds for finite ele-

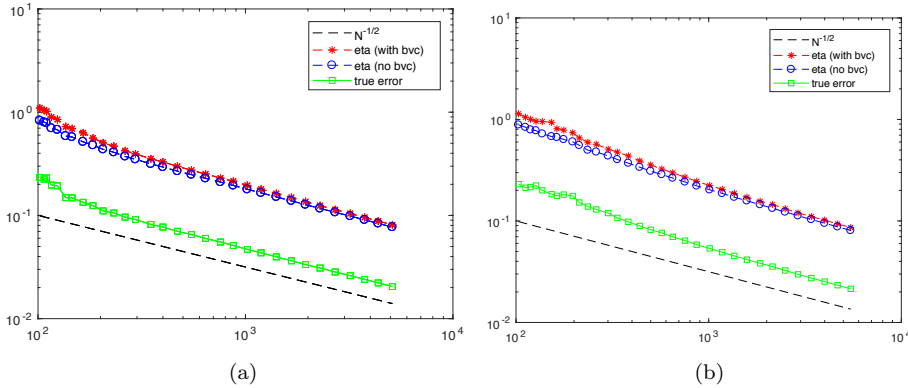


FIG. 10. Estimator convergence performance without and with $\|\nabla\tilde{e}\|$. Left: $\omega = 31\pi/8$. Right: $\omega = 63\pi/16$.

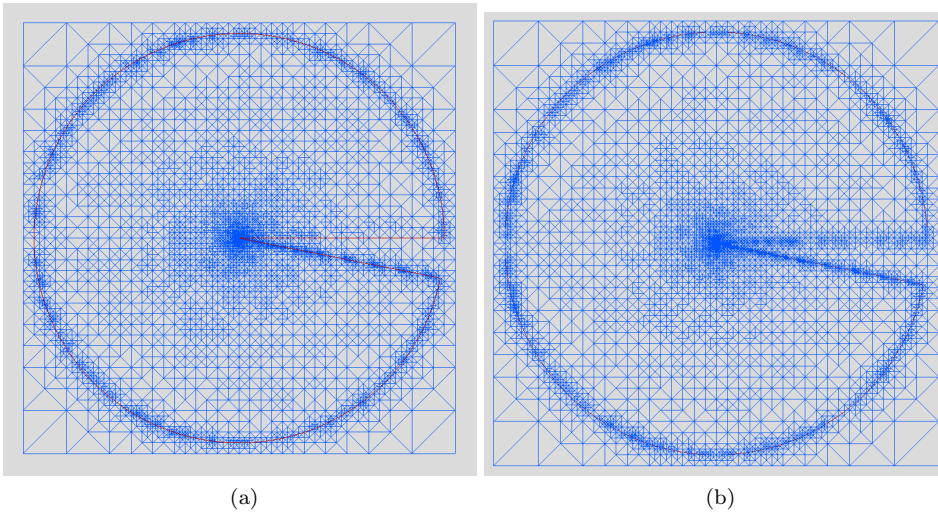


FIG. 11. Final meshes without and with $\|\nabla\tilde{e}\|$.

ment approximation on nonpolygonal domains. *IMA Journal of Numerical Analysis*, **37**(2), 604–645.

Barrett, John W., & Elliott, Charles M. 1984. A finite-element method for solving elliptic equations with Neumann data on a curved boundary using unfitted meshes. *IMA J. Numer. Anal.*, **4**(3), 309–325.

Becker, Roland, Burman, Erik, & Hansbo, Peter. 2011. A hierarchical NXFEM for fictitious domain simulations. *Internat. J. Numer. Methods Engrg.*, **86**(4-5), 549–559.

Bernland, A., Wadbro, E., & Berggren, M. 2018. Acoustic shape optimization using cut finite elements. *Internat. J. Numer. Methods Engrg.*, **113**(3), 432–449.

Bertoluzza, S., Ismail, M., & Maury, B. 2005. The fat boundary method: semi-discrete scheme and some numerical experiments. *Pages 513–520 of: Domain decomposition methods in science and engineering*. Lect. Notes Comput. Sci. Eng., vol. 40.

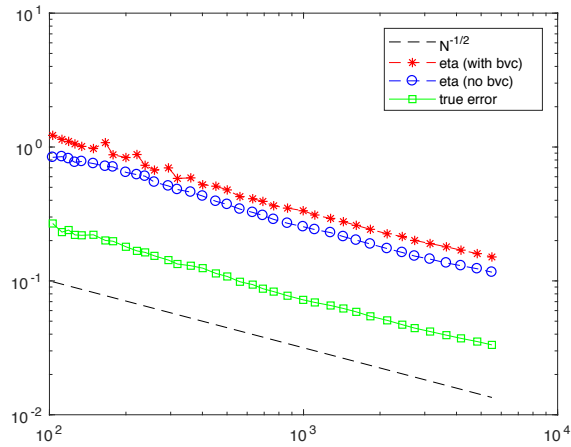


FIG. 12. Convergence performance for estimator without and with boundary correction.

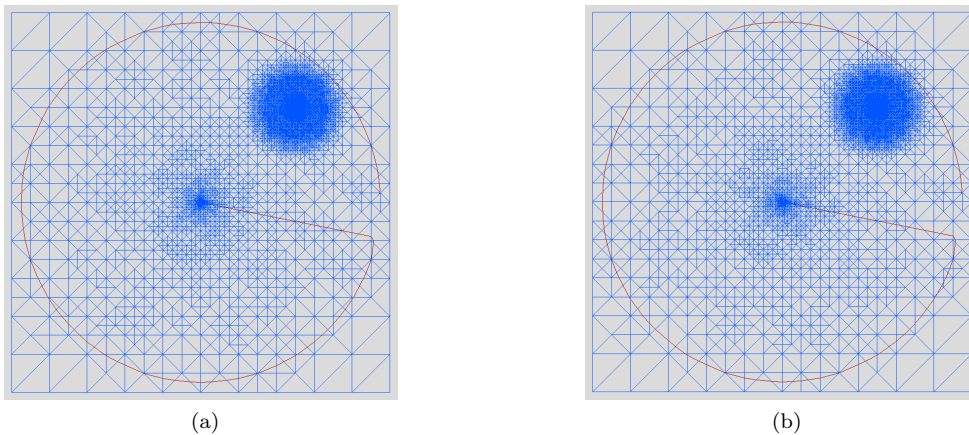


FIG. 13. Final meshes generated without (left) and with (right) $\|\nabla\tilde{e}\|_K$.

Springer, Berlin.

Boiveau, T., Burman, E., Claus, S., & Larson, M. 2018. Fictitious domain method with boundary value correction using penalty-free Nitsche method. *J. Numer. Math.*, **26**(2), 77–95.

Bramble, James H., & King, J. Thomas. 1994. A robust finite element method for nonhomogeneous Dirichlet problems in domains with curved boundaries. *Math. Comp.*, **63**(207), 1–17.

Bui, H. P., Tomar, S., & Bordas, S. P. A. 2019. Corotational cut finite element method for real-time surgical simulation: application to needle insertion simulation. *Comput. Methods Appl. Mech. Engrg.*, **345**, 183–211.

Burman, E. 2010. Ghost penalty. *C. R. Math. Acad. Sci. Paris*, **348**(21-22), 1217–1220.

Burman, E., & Ern, A. 2019. A cut cell hybrid high-order method for elliptic problems with curved boundaries. *Pages 173–181 of: European Conference on Numerical*

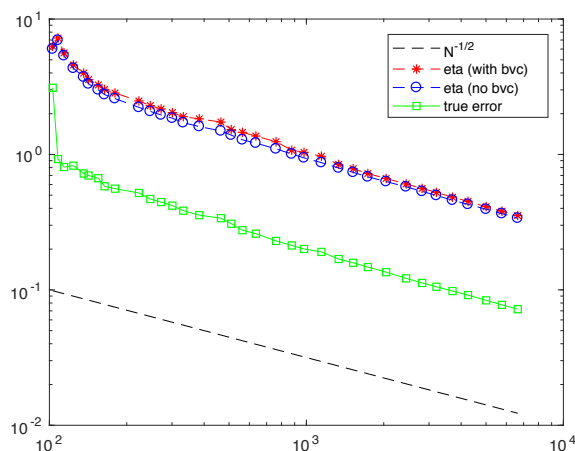


FIG. 14. Convergence performance for estimator without and with $\|\nabla\bar{e}\|$.

- Mathematics and Advanced Applications, ENUMATH 2017; Voss; Norway.* Lecture Notes in Computational Science and Engineering, vol. 126.
- Burman, E., & Hansbo, P. 2010. Fictitious domain finite element methods using cut elements: I. A stabilized Lagrange multiplier method. *Comput. Methods Appl. Mech. Engrg.*, **199**(41-44), 2680–2686.
- Burman, E., & Hansbo, P. 2012. Fictitious domain finite element methods using cut elements: II. A stabilized Nitsche method. *Appl. Numer. Math.*, **62**(4), 328–341.
- Burman, E., & Hansbo, P. 2014. Fictitious domain methods using cut elements: III. A stabilized Nitsche method for Stokes' problem. *ESAIM Math. Model. Numer. Anal.*, **48**(3), 859–874.
- Burman, E., Claus, S., & Massing, A. 2015a. A stabilized cut finite element method for the three field Stokes problem. *SIAM J. Sci. Comput.*, **37**(4), A1705–A1726.
- Burman, E., Elfverson, D., Hansbo, P., Larson, M. G., & Larsson, K. 2017. A cut finite element method for the Bernoulli free boundary value problem. *Comput. Methods Appl. Mech. Engrg.*, **317**, 598–618.
- Burman, E., Hansbo, P., & Larson, M. G. 2018a. A cut finite element method with boundary value correction. *Math. Comp.*, **87**(310), 633–657.
- Burman, E., Elfverson, D., Hansbo, P., Larson, M. G., & Larsson, K. 2018b. Shape optimization using the cut finite element method. *Comput. Methods Appl. Mech. Engrg.*, **328**, 242–261.
- Burman, Erik, Claus, Susanne, Hansbo, Peter, Larson, Mats G., & Massing, André. 2015b. CutFEM: discretizing geometry and partial differential equations. *Internat. J. Numer. Methods Engrg.*, **104**(7), 472–501.
- Cai, Zhiqiang, He, Cuiyu, & Zhang, Shun. 2017. Residual-based a posteriori error estimate for interface problems: Nonconforming linear elements. *Mathematics of Computation*, **86**(304), 617–636.
- Di Pietro, D. A., & Ern, A. 2012. *Mathematical aspects of discontinuous Galerkin methods*. Mathématiques & Applications (Berlin) [Mathematics & Applications], vol. 69. Springer, Heidelberg.
- Dörfler, Willy, & Rumpf, Martin. 1998. An adaptive strategy for elliptic problems including a posteriori controlled boundary approximation. *Mathematics of Compu-*

- tation of the American Mathematical Society*, **67**(224), 1361–1382.
- Elfverson, D., Larson, M. G., & Larsson, K. 2018. CutIGA with Basis Function Removal. *arXiv e-prints*, Jan.
- Embar, Anand, Dolbow, John, & Harari, Isaac. 2010. Imposing Dirichlet boundary conditions with Nitsche’s method and spline-based finite elements. *Internat. J. Numer. Methods Engrg.*, **83**(7), 877–898.
- Glowinski, R., & Pan, T.-W. 1992. Error estimates for fictitious domain/penalty/finite element methods. *Calcolo*, **29**(1-2), 125–141 (1993).
- Grisvard, Pierre. 2011. *Elliptic problems in nonsmooth domains*. Classics in Applied Mathematics, vol. 69. Society for Industrial and Applied Mathematics (SIAM), Philadelphia, PA. Reprint of the 1985 original [MR0775683], With a foreword by Susanne C. Brenner.
- Gürkan, Ceren, & Massing, André. 2019. A stabilized cut discontinuous Galerkin framework for elliptic boundary value and interface problems. *Computer Methods in Applied Mechanics and Engineering*, **348**, 466–499.
- Guzmán, J., & Olshanskii, M. 2018. Inf-sup stability of geometrically unfitted Stokes finite elements. *Math. Comp.*, **87**(313), 2091–2112.
- Hansbo, Anita, & Hansbo, Peter. 2002. An unfitted finite element method, based on Nitsche’s method, for elliptic interface problems. *Comput. Methods Appl. Mech. Engrg.*, **191**(47-48), 5537–5552.
- Hansbo, P., Larson, M. G., & Zahedi, S. 2015. Characteristic cut finite element methods for convection-diffusion problems on time dependent surfaces. *Comput. Methods Appl. Mech. Engrg.*, **293**, 431–461.
- Hansbo, Peter, Larson, Mats G, & Larsson, Karl. 2017. Cut finite element methods for linear elasticity problems. *Pages 25–63 of: Geometrically Unfitted Finite Element Methods and Applications*. Springer.
- Haslinger, J., & Renard, Y. 2009. A new fictitious domain approach inspired by the extended finite element method. *SIAM J. Numer. Anal.*, **47**(2), 1474–1499.
- Johansson, A., & Larson, M. G. 2013. A High Order Discontinuous Galerkin Nitsche Method for Elliptic Problems with Fictitious Boundary. *Numer. Math.*, **123**(4), 607–628.
- Jonsson, Tobias, Larson, Mats G, & Larsson, Karl. 2019. Graded parametric Cut-FEM and CutIGA for elliptic boundary value problems in domains with corners. *Computer Methods in Applied Mechanics and Engineering*.
- Lehrenfeld, C. 2017. A higher order isoparametric fictitious domain method for level set domains. *Pages 65–92 of: Geometrically Unfitted Finite Element Methods and Applications*. Lect. Notes Comput. Sci. Eng., vol. 121. Springer, Cham.
- Massing, A., Larson, M. G., Logg, A., & Rognes, M. E. 2014a. A stabilized Nitsche fictitious domain method for the Stokes problem. *J. Sci. Comput.*, **61**(3), 604–628.
- Massing, A., Schott, B., & Wall, W. A. 2018. A stabilized Nitsche cut finite element method for the Oseen problem. *Comput. Methods Appl. Mech. Engrg.*, **328**, 262–300.
- Massing, André, Larson, Mats G., Logg, Anders, & Rognes, Marie E. 2014b. A stabilized Nitsche fictitious domain method for the Stokes problem. *J. Sci. Comput.*, **61**(3), 604–628.
- Nitsche, J. 1971. Über ein Variationsprinzip zur Lösung von Dirichlet-Problemen bei Verwendung von Teilräumen, die keinen Randbedingungen unterworfen sind. *Abh. Math. Sem. Univ. Hamburg*, **36**, 9–15. Collection of articles dedicated to Lothar Collatz on his sixtieth birthday.
- Schott, B., & Wall, W. A. 2014. A new face-oriented stabilized XFEM approach for

- 2D and 3D incompressible Navier-Stokes equations. *Comput. Methods Appl. Mech. Engrg.*, **276**, 233–265.
- Schott, B., Shahmiri, S., Kruse, R., & Wall, W. A. 2016. A stabilized Nitsche-type extended embedding mesh approach for 3D low- and high-Reynolds-number flows. *Internat. J. Numer. Methods Fluids*, **82**(6), 289–315.
- Scott, L Ridgway, & Zhang, Shangyou. 1990. Finite element interpolation of non-smooth functions satisfying boundary conditions. *Mathematics of Computation*, **54**(190), 483–493.
- Swift, L. 2018. *Geometrically unfitted finite element methods for the Helmholtz equation*. Ph.D. thesis, University College London.
- Verfürth, Rüdiger. 1994. A posteriori error estimation and adaptive mesh-refinement techniques. *Journal of Computational and Applied Mathematics*, **50**(1-3), 67–83.
- Winter, M., Schott, B., Massing, A., & Wall, W. A. 2018. A Nitsche cut finite element method for the Oseen problem with general Navier boundary conditions. *Comput. Methods Appl. Mech. Engrg.*, **330**, 220–252.